Journal of
Nanoscience and Nanotechnology
Vol. 11, 5904–5908, 2011

RESEARCH ARTICLE

Fluorination of Aluminum Oxide Gate Dielectrics Using Fluorine Neutral/Ion Beams

Byoung Jae Park[1], Woong Sun Lim[2], Jae Kwan Yeon[1], Yi Yeon Kim[1], Se Koo Kang[2], Jong Tae Lim[1], and Geun Young Yeom[1, 2, *]

[1] *Department of Advanced Materials Engineering, Sungkyunkwan University, Suwon, 440-746, South Korea*
[2] *SKKU Advanced Institute of Nano Technology, Sungkyunkwan University, Suwon, 440-746, South Korea*

The effect of the fluorination of aluminum oxide (Al_2O_3) in an oxide-nitride-aluminum oxide (SiO_2–Si_3N_4–Al_2O_3, ONA) layer through fluorine (F) ion and neutral-beam treatments on the characteristics of the ONA layer was investigated to study the effect of charge-related damage during F ion beam treatment. The treatment with an F beam at ~10 eV energy produced an about-5-nm-thick fluorinated alumina layer by replacing the aluminum–oxygn (Al–O) bonding with Al–F bonding for both the F neutral-beam and F ion beam treatments. Moreover, no significant differences in the physical and chemical properties of the ONA layers treated with the two beams were observed. When the electrical characteristics of the metal-oxide-semiconductor (MOS) devices were compared, however, the lowest leakage current and highest memory window characteristics were observed in the MOS device fabricated with an F neutral beam, due to the Al–F layer formed on the Al_2O_3 surface. In the case of the MOS device fabricated with the F-ion-beam-treated ONA layer, however, lower electrical characteristics were observed compared to the MOS device fabricated with the F-neutral-beam-treated ONA layer, possibly due to the charge-related damage that occurred during the F ion beam treatment, even though the memory characteristics were improved compared to the reference due to the Al–F layer formed on the Al_2O_3 surface.

Keywords: Fluorine (F) Neutral Beam, Fluorination, Floating Gate Dielectric, Al_2O_3.

1. INTRODUCTION

For the next-generation nanoscale volatile- and nonvolatile-memory devices, materials more advanced than silicon oxide (SiO_2) are required for the gate dielectrics because the SiO_2 gate dielectric is approaching both its technological and theoretical limits.[1, 2] Especially, these days, flash memory devices such as the silicon-oxide-nitride-oxide-silicon (SONOS) devices, which utilize charge trapping at the gate dielectric for nonvolatile-memory storage, have received much attention as mass storage electronic equipment. In these devices, increasing the capacity of the gate dielectrics is the most important objective.

Various high-*k* dielectric materials are currently being investigated, and among these, aluminum oxide (Al_2O_3) shows the best dielectric properties, such as a high dielectric constant and a lower leakage current at an equivalent SiO_2 thickness, even though it has problems regarding its electrical properties (e.g., interface charges, capacitance frequency dispersion, etc.) that still need to be addressed.[3–6] One of the techniques that have been used to resolve these problems is the fluorination of Al_2O_3 via fluorine (F) ion implantantion, F plasma treatment, etc., to improve the electrical properties of Al_2O_3. It has been reported that fluorination improves the electrical properties and reliability of the dielectric materials, including Al_2O_3.[7–10]

The fluorination of Al_2O_3 for SONOS devices was previously investigated by treating Al_2O_3 using a low-energy F neutral beam. The results showed that the fluorination of Al_2O_3 with an F neutral beam can lower the leakage current and significantly improve the memory window characteristics of SONOS devices.[11] As the F neutral beam is a chargeless F particle beam, the improved electrical properties of Al_2O_3 treated with an F neutral beam may be partly due to the fact that no charge-related damage occurred during the F neutral-beam treatment of Al_2O_3.

Even though the previous study showed the effect of the F neutral beam on the electrical characteristics of the oxide-nitride-aluminum oxide (SiO_2–Si_3N_4–Al_2O_3, ONA) gate dielectric stack, F neutral-beam treatment has not

*Author to whom correspondence should be addressed.

 1533-4880/2011/11/5904/005 doi:10.1166/jnn.2011.4359

been compared with the conventional F plasma treatments, such as the treatment using an F ion beam. Therefore, in this study, F beam treatment was carried out on the Al_2O_3 layer of an ONA gate dielectric stack, using an F neutral beam and an F ion beam, to improve of the electrical properties (e.g., charge-trapping properties) of SONOS-type floating-gate-memory devices. Moreover, the effects of F beam treatment with an F neutral beam and an F ion beam on the physical and chemical characteristics of the Al_2O_3 gate dielectric material and on the electrical characteristics of the ONA structure, such as the leakage current and the hysteresis of the capacitance–voltage, due to the fluorination of Al_2O_3, were compared.

2. EXPERIMENTAL DETAILS

An ONA gate dielectric stack layer was formed on *p*-type (100) silicon as a fluorination sample. 4-nm-thick SiO_2 was grown thermally, 7-nm-thick Si_3N_4 was deposited via low-pressure chemical vapor deposition, and 15-nm-thick Al_2O_3 was deposited via atomic-layer deposition, in sequence, on the silicon wafer. After the formation of the ONA layer on the silicon wafer, post-deposition rapid thermal annealing was performed at 1080 °C for 2 min, in a N_2 ambient.

The Al_2O_3 of the ONA layer, which is used as a charge-blocking layer, was fluorinated using an F ion beam and an F neutral beam. Figure 1 shows the schematic diagrams of the F ion and neutral-beam systems that were used for the fluorination. For the extraction of the F beam, a 6-inch-diameter, three-grid inductively coupled plasma (ICP) source was used. The ICP source was operated at 300 W, with a 13.56 MHz rf power supply, and 30 sccm NF_3 was flown to the source to generate F ions. F ions with a low energy of ~10 eV were formed by applying +10 and −700 V to the first grid (located close to the ICP source) and the second grid, respectively, while the third grid (located close to the reflector) was grounded. To form an F neutral beam, as shown in Figure 1, a parallel stack of graphite plates tilted by about 5° towards the direction of the ion beam was installed in front of the ICP ion gun for the neutralization of the F ion during the reflection of the extracted F ion beam on the reflector. More details regarding the beam source can be found elsewhere.[12–14] Therefore, by installing or removing the reflector stack in front of the 6-inch-diameter ICP ion gun, the source was operated as an F neutral- beam or ion beam source, respectively.

The Al_2O_3 of the ONA layer on *p*-type (100) silicon was treated with an F neutral or F ion beam for 15 min. After the beam treatment, a metal-oxide-semiconductor (MOS) device was fabricated to measure the electrical properties of the ONA layer on the *p*-type (100) silicon wafer. To form the MOS device structure, a 50×50-μm^2, 100-nm-thick Pt electrode was deposited via dc sputtering on the top and bottom of the samples, as the gate electrodes, followed by forming gas annealing (FGA) at 400 °C for 30 min.

The distribution of F atoms in Al_2O_3, produced by the F beam treatment, was measured, and the Al bonding state on the surface of the fluorinated Al_2O_3 thin film was analyzed, via X-ray photoelectron spectroscopy (XPS, VG Microtech Inc. ESCA2000). Atomic-force microscopy (AFM, Thermomicroscopes Autoprobe CT) was used to analyze the surface morphology of the Al_2O_3 thin film after the fluorination procedure. The thickness of the fluorinated Al_2O_3 layer was observed with a transmission electron microscope (TEM, JEOL JEM 2100F). Finally, the high-frequency (100 kHz) capacitance–voltage (C–V) and current–voltage (I–V) curves were measured using HP4284A and HP4155C semiconductor parameter analyzers, respectively.

3. RESULTS AND DISCUSSION

Figure 2 shows the XPS depth profiles of the fluorine (F), oxygen (O), and aluminum (Al) in the ONA layers treated

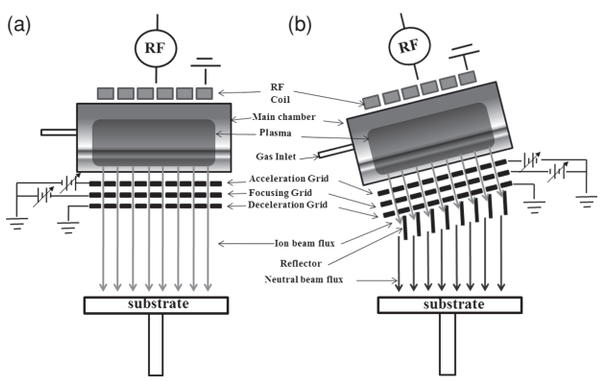

Fig. 1. Schematic diagrams of the (a) F ion beam system and (b) F neutral-beam system used in the experiment.

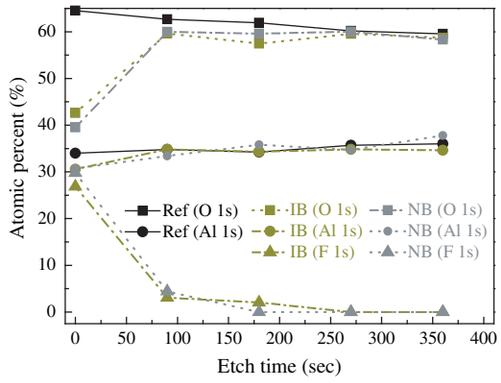

Fig. 2. XPS depth profiles of the F, O and Al atomic distributions in the F-neutral- and F-ion-beam-treated ONA layers. The XPS depth profile of the untreated ONA layer was included as a reference.

with low-energy F neutral/ion beams, respectively. The XPS depth profiles of the F, O, and Al in the ONA layers before the F beam treatment were included as references. For XPS depth profiling, a 3 kV and 2uA argon (Ar) beam was used. As shown in Figure 2, after the low-energy F ion beam and F neutral-beam treatment, the penetration of F into Al_2O_3 was observed. The maximum amount of F was observed to have penetrated into Al_2O_3, rapidly decreasing with the increasing depth of Al_2O_3, and reaching the minimum amount after a sputter etch time of about 275 sec for both treatments. The fact that the maximum amount of F was observed on the surface is believed to be due to the low-energy F beam treatments that were used in the experiment. In the case of the O XPS depth profile, it increased with increasing profiling depth and reached the maxiumum after about 275 sec. As for the Al XPS peak, no change in the composition with the depth was observed in either of the treated samples. When the XPS depth profiles of O and Al for the Al_2O_3 layers treated and untreated with an F beam were compared, the loss of O on the surface of Al_2O_3 due to the F beam treatment was seen. Therefore, due to the F beam treatment, some of the O in the Al_2O_3 appeared to have been replaced by F in both treated samples. When the chemical-binding state of Al on the Al_2O_3 surface after the F beam treatments was investigated via XPS, the samples that were treated with both the F neutral and F ion beams showed a peak at 76.7 eV related to Al–F bonding, in addition to the peak at 74.2 eV related to Al–O bonding. In addition, the intensity of the Al–O bonding peak decreased after the formation of Al–F bonding. Al–F bonding thus appeared to have been formed by the replacement of the Al–O bonding during the F beam treatments of the Al_2O_3 layers on the ONA layers (not shown).

Figure 3 shows the cross-sectional TEM images of the ONA layers for the (a) untreated ONA layer, (b) F-ion-beam-treated ONA layer, and (c) F-neutral-beam-treated ONA layer. As shown in Figure 3(a), a total ONA thickness of 26 nm (15 nm: Al_2O_3; 7 nm: Si_3N_4; 4 nm: SiO_2) on the silicon wafer was confirmed for the untreated ONA layer. Even after the F beam treatment with the neutral and ion beams, the total thickness of the ONA stack remained close to 26 nm, as shown in Figure 3(b) and (c), respectively, indicating that there was no observable etching of the Al_2O_3 layer during the low-energy F beam treatments. After both F beam treatments, however, a change in the Al_2O_3 surface of the ONA layer (i.e., Al_2O_3's thickness decreased to about 5 nm) was observed for both treatmenents.

The surface roughnesses of the ONA layers before and after fluorination with an F neutral or ion beam were investigated via AFM (scan area: 3×3 um; three-time scan), and the results are shown in Figure 4 and Table I. As shown in the table, the rms surface roughness of the untreated sample was 0.35 ± 0.05 nm, while those

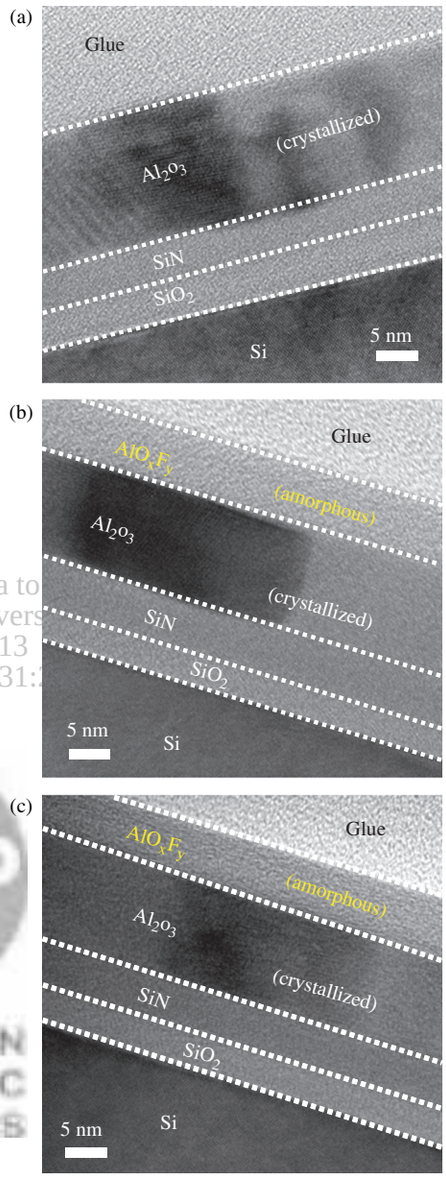

Fig. 3. Cross-sectional TEM images of the ONA layers: (a) untreated ONA layer; (b) F-ion-beam-treated ONA layer; and (c) F-neutral-beam-treated ONA layer.

of the F-ion- and F-neutral-beam-treated samples were 0.25 ± 0.04 and 0.24 ± 0.04 nm, respectively. Therefore, F beam treatment appeared to have slightly improved the surface roughness of the ONA layers, and no difference between the F ion beam and F neutral-beam treatments was observed in this regard.

Using the ONA layers on the silicon wafers treated with the F neutral/ion beams, MOS devices were fabricated, as described in the "Experimental Details" section, to measure the electrical properties of the ONA layers. The *I–V* characteristics of the fabricated MOS devices are shown in Figure 5. For reference, the *I–V* characteristics of the MOS device fabricated with the untreated ONA layer are

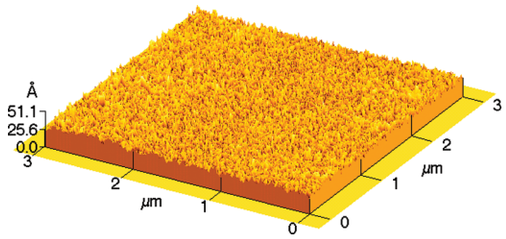

(a) Reference (RMS = 0.35 nm)

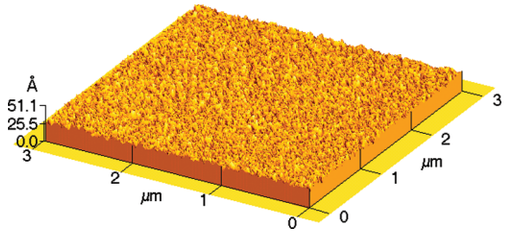

(b) NF_3 neutral beam (RMS = 0.24 nm)

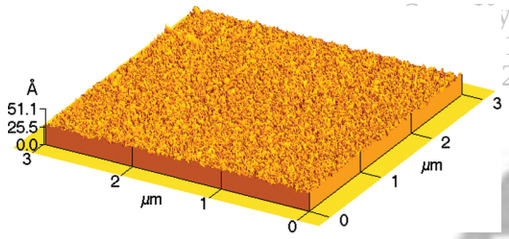

(c) NF_3 ion beam (RMS = 0.25 nm)

Fig. 4. AFM images and rms surface roughnesses of the ONA layers: (a) Reference; (b) F-netral-beam-treatment ONA layer; and (c) F-ion-beam-treated ONA layer. The treatment time was 15 min.

also shown. The *I–V* characteristics of the MOS device with the ONA layer showed three distinct regions (from 0 to −2 V, from −2 to −12 V, and above −12 V), which may be related to the breakdown of each material in the ONA layer at the respective voltages. The operating voltages of the SONOS device were 0 to −10 V. Even though no significant differences were observed among the MOS devices, the F-neutal beam-treated MOS device showed the lowest leakage current among the MOS devices fabricated in this study. In the case of the MOS device treated with the F ion beam, a slightly higher leakage current in the regions of 0 to −2 V and above −12 V was observed. Therefore, the F ion beam treatment appeared to have

Table I. AFM images and rms surface roughnesses of the ONA layers: (a) Reference; (b) F-neutral-beam-treated ONA layer; and (c) F-ion-beam treated ONA layer (AFM scan area: 3 × 3 um; three-time scan). The treatment time was 15 min.

	Reference	NF_3 neutral beam treatment	NF_3 ion beam treatment
RMS roughness	0.35 nm ± 0.04	0.24 nm ± 0.04	0.25 nm ± 0.04

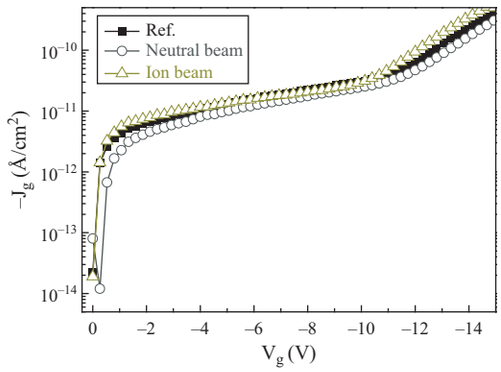

Fig. 5. *I–V* characteristics of the MOS devices fabricated with the ONA layers treated with the F neutral/ion beams. The *I–V* characteristics of the device with the untreated ONA layer were included as references.

caused charge-related damage, even though the samples were made to undergo FGA at 400 °C for 30 min after the deposition of the gate electrodes.

The *C–V* characteristics of the MOS devices described above were also measured, and the results are shown in Figure 6. The *C–V* characteristics of the MOS devices showed a hystesis curve (related to the memory window characteristics) within the voltage range of −15∼15 V, due to the charge trapping between Si_3N_4 and Al_2O_3 in the ONA layers. As shown in the *C–V* hysteresis curve, the MOS device fabricated with the F-neutral-beam-treated ONA layer showed the widest memory window characteristics due to the increase in its charge-trapping characteristics. When the *C–V* characteristics of the MOS device fabricated with the F-neutral-beam-treated ONA layer were compared with those of the MOS device fabraicated with the untreated ONA layer, the charge-trapping characteristics related to electron trappling were found to have been significantly improved for the MOS device fabricated with the F-neutral-beam-treated ONA layer. This is believed to be related to the effective electron blocking

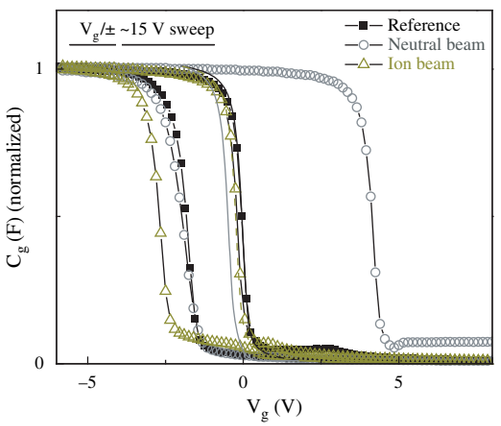

Fig. 6. *C–V* hysteresis curves of the MOS devices fabricated with the ONA layers treated with the F neutral/ion beams. The *C–V* curve of the device with the untreated ONA layer was included as a reference.

by the Al–F layer formed on the surface of the Al_2O_3 without causing any charge-related damage. In the case of the *C–V* characteristics of the MOS device fabricated with the F-ion-beam-treated ONA layer, the memory window was also improved compared with that of the MOS device fabricated with the untreated ONA layer, due to the Al–F layer formed on the Al_2O_3. The memory window, however, was narrower than that of the MOS device fabricated with the F-neutral-beam-treated ONA layer. Moreover, the improvement of the memory window was related to hole trapping rather than to electron trappling, which might be due to the positive-charge-related damage during the F ion bombardment. The charge-related damage to the ONA layer during the F ion beam treatment needs to be investigated in detail, but the significant differences in the characteristics of the MOS device due to the charging of the ONA layer were confirmed by measuring the *C–V* characteristics of the MOS devices, and a significant improvement of the memory characteristics of the MOS device fabricated with the F-neutral-beam-treated ONA layer was observed.

4. CONCLUSIONS

In this study, the effects of low-energy (10 eV) fluorine (F) beam (ion/neutral beam) treatment of the Al_2O_3 of an oxide-nitride-aluminum oxide (SiO_2–Si_3N_4–Al_2O_3, ONA) layer on the physical, chemical, and electrical characteristics of the ONA layer were compared to investigate the effect of the charge-related damage incurred during the F beam treatment of SONOS devices. The treatment with the F beam at ~10 eV energy resulted in the fluorination of the surface of the about-5-nm-thick Al_2O_3 by replacing the Al–O bonding with Al–F bonding without changing the total thickness of the ONA layer. After the 15-min F neutral-beam and ion beam treatments, the surface roughnesses of the ONA layers changed from 0.345 nm to about 0.246 and 0.244 nm, respectively. Therefore, no significant differences in the physical and chemical properties of the F-ion- and F-neutral-beam-treated ONA layers were observed. When the electrical characteristics (e.g., *I–V* and *C–V* characteristics) of the MOS devices fabricated with the F-ion- and F-neutral-beam-treated ONA layers were compared, however, the *I–V* and *C–V* characteristics were found to be superior after the F neutral-beam treatment, possibly due to the defect passivation by the incorporation of F into the Al_2O_3 layer and the enhanced electron trapping by the Al–F layer formed on the surface of Al_2O_3 without any charge-related damage incurred during the F beam treatment. On the other hand, the slightly increased leakage current compared to that of the reference, and the limited improvement of the *C–V* characteristics obtained after the F ion beam treatment, appear to be related to the charge-related damage that was incurred during the F ion beam treatment, even when an Al–F layer was formed on the surface of the Al_2O_3 layer.

Acknowledgments: This work was supported by the National Research Foundation of Korea Grant funded by the Korean Government (MEST) (NRF-2010-M1AWA001-2010-0026248) and the IT R&D program of MKE/KEIT [10030694, International Collaborative R&D Project for semiconductor].

References and Notes

1. M. Schulz, *Nature* 399, 729 (**1999**).
2. P. A. Packan, *Science* 285, 2079 (**1999**).
3. E. Gusev, M. Copel, E. Cartier, I. J. R. Baumvol, C. Krug, and M. A. Gribelyuk, *Appl. Phys. Lett.* 76, 176 (**2000**).
4. J. Robertson, *J. Vac. Sci. Technol. B* 18, 1785 (**2000**).
5. S. W. Lee, K. J. Chung, I. S. Park, and J. H. Ahn, *J. Nanosci. Nanotechnol.* 9, 6974 (**2009**).
6. Y. Kim, S. M. Lee, C. S. Park, S. I. Lee, and M. Y. Lee, *Appl. Phys. Lett.* 71, 3604 (**1997**).
7. M. Inoue, S. Tsujikawa, M. Mizutani, K. Nomura, T. Hayashi, K. Shiga, J. Yugami, J. Tsuchimoto, Y. Ohno, and M. Yoneda, *IEDM Tech. Dig.* 413 (**2005**).
8. C. S. Lai, W. C. Wu, J. C. Wan, and T. S. Chaos, *Appl. Phys. Lett.* 86, 222905 (**2005**).
9. P. J. Wright and K. C. Saraswat, *IEEE Trans. Electron Devices* 36, 879 (**1989**).
10. C. H. Lee, S. H. Hur, Y. C. Shin, J. H. Choi, D. G. Park, and K. N. Kim, *Appl. Phys. Lett.* 86, 152908 (**2005**).
11. S. W. Kim, B. J. Park, S. K. Kang, B. H. Kong, H. K. Cho, G. Y. Yeom, S. H. Heo, and H. W. Hwang, *Appl. Phys. Lett.* 93, 191506 (**2008**).
12. B. J. Park, S. W. Kim, S. K. Kang, K. S. Min, S. D. Park, S. J. Kyung, H. C. Lee, J. W. Bae, J. T. Lim, D. H. Lee, and G. Y. Yeom, *J. Phys. D.* 41, 024005 (**2008**).
13. W. S. Lim, J. B. Park, J. Y. Park, B. J. Park, and G. Y. Yeom, *J. Nanosci. Nanotechnol.* 9, 7379 (**2009**).
14. K. S. Min, B. J. Park, J. B. Park, S. K. Kang, and G. Y. Yeom, *J. Korean. Phys. Soc.* 51, 967 (**2007**).

Received: 12 July 2010. Accepted: 25 January 2011.